CDF/ANAL/TOP/CDFR/8181
Version 1.0
March 27, 2006

Measurement of the $W^{\pm} + b\bar{b}$ Cross-Section

Mitch Soderberg, Dave Gerdes
University of Michigan

Chris Neu
University of Pennsylvania

Abstract

In this note we report the results of the $W^{\pm}+b\bar{b}$ cross-section analysis using 695 pb^{-1} of integrated luminosity in the `bhel0d`, `bhmu0d`, `bhel0h`, and `bhmu0h` data samples. Our method relies on fits of the invariant mass of SECVTX tagged jets in the lepton+jets data sample to isolate the contribution of b-decays. A combination of data and MC is used to turn the measured b-fraction of these tagged jets into the cross-section for $W^{\pm}+b\bar{b}$ production. We have measured the inclusive $W^{\pm}+b\bar{b}$ cross-section times branching ratio to leptons for the first time at CDF, obtaining 4.46±1.13(stat.)±1.64(syst.)pb. This is to be compared with the theoretical prediction of 3.8±0.9pb.

Contents

1 Introduction

$W^{\pm} + b\bar{b}$ refers to the production of events that contain a $W^{\pm}$ boson, a pair of b-quarks ($b\bar{b}$) which are almost entirely produced by gluon splitting, and any number of additional partons. The leading-order (LO) diagram is depicted in Figure 1. This is an important and challenging process that must be accounted for since it is a background source in MSSM Higgs searches, single-top searches, and the $t\bar{t}$ cross-section analysis.

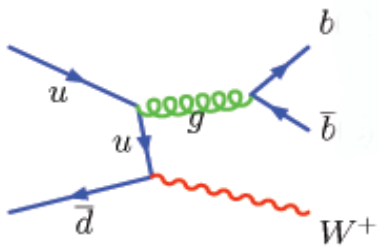

Figure 1: Leading order Feynman diagram for $W^{\pm} + b\bar{b}$ production.

The difficulty in analyzing $W^{\pm} + b\bar{b}$ is largely due to its QCD nature. The theoretically predicted rate of $W^{\pm} + b\bar{b}$ production is very dependent on the choice of renormalization and factorization scales that its Feynman diagrams are evaluated at. Furthermore, the fact that $W^{\pm} + b\bar{b}$ is approximated by the LO diagrams in its perturbation expansion when producing monte carlo (MC) samples could lead to large theoretical uncertainty in the predictions of those samples[1]. The presence of extra partons in the matrix-element diagrams introduces ambiguity due to the manner in which we utilize a MC generator to make event samples for different multiplicities (*i.e.* - $W^{\pm}+b\bar{b}$+0p, $W^{\pm}+b\bar{b}$+1p, $W^{\pm}+b\bar{b}$+2p), and then we shower these events with Herwig or Pythia. The addition of extra partons, beyond those present in the matrix-element, during the showering process can cause identical events to be produced in the different parton multiplicity samples, which could lead to double-counting of certain regions of phase-space. All of these issues make it very difficult to precisely estimate the contribution of $W^{\pm} + b\bar{b}$ to our data and give us reason to pursue a measurement of this process that relies as much on the data as possible.

This note describes the measurement of the $W^{\pm} + b\bar{b}$ cross-section for the first time at CDF, using 695 pb^{-1} of integrated luminosity in the `bhel0d`, `bhmu0d`, `bhel0h`, and `bhmu0h` data samples. This is an extension of the earlier measurement of the ratio of the observed $W^{\pm} + b\bar{b}$ cross-section ($\sigma'_{W^{\pm}+b\bar{b}}$) to the observed $W^{\pm}$+jets cross-section ($\sigma_{W^{\pm}+1,2j}$) in the 1 and 2 jet bins of the Lepton+Jets data[2]. In that analysis no attempt was made to correct the estimates of $W^{\pm} + b\bar{b}$ and $W^{\pm} + 1, 2j$ back to the true number of these processes present in the data. That method allowed for a comparison

with the heavy-flavor fractions of the Method II analysis, but not with a theoretical prediction of $W^{\pm}+b\bar{b}$ production.

We need to isolate $W^{\pm}+b\bar{b}$ in the data in order to measure its cross-section. We use the SECVTX mass of tagged jets in the 1 and 2 jet bins of the data to distinguish tags due to bottom, charm, and mistags. Once we know how many tagged jets in the data are due to b-decays, we account for any non-$W^{\pm}+b\bar{b}$ contribution to this total, leaving only the number of tagged b-decays from $W^{\pm}+b\bar{b}$. Dividing this number by the average number of tags in a 1 or 2 jet $W^{\pm}+b\bar{b}$ event gives us the number of $W^{\pm}+b\bar{b}$ events in the 1 or 2 jet bins of the pretag data. Finally, we use efficiency and acceptance factors to correct this number of pretag $W^{\pm}+b\bar{b}$ events in the 1+2 jet bins back to the true number of $W^{\pm}+b\bar{b}$ events that should have been initially produced in the data sample.

1.1 Cross-Section Definition

In this analysis we have tried to account for all efficiency and acceptance factors in order to produce a measurement of the true physics-level cross-section for $W^{\pm}+b\bar{b}$ production. The cross-section is defined to be inclusive, meaning that any number of additional partons are allowed in the matrix-element diagrams (beyond the $b\bar{b}$ pair). Since we are using a matrix-element generator to produce event samples and theoretical cross-sections, we employ a minimal set of cuts on the partons and leptons of the matrix-elements in order to increase the efficiency of the generation (in terms of CPU) but still provide modeling of all possible $W^{\pm}+b\bar{b}$ events that can make it into the data. This makes our results not completely inclusive (due to the phase-space we're explicitly not generating), but we've shown elsewhere that the removed phase-space contributes very little to the data[3].

We write the inclusive cross-section generically as:

$$\sigma_{W^{\pm}+b\bar{b}} = \frac{N_{W^{\pm}+b\bar{b}}}{\mathcal{L}} \tag{1}$$

where $N_{W^{\pm}+b\bar{b}}$ is the true number of $W^{\pm}+b\bar{b}$ events produced in the integrated luminosity, $\mathcal{L}$, of our data sample. As in the previous version of the analysis we move to a cross-section defined in terms of the observed number of $W^{\pm}+b\bar{b}$ events in the 1+2 jet bins of the pretag sample, $N'_{W^{\pm}+b\bar{b}}$, as shown in Eq. 2.

$$\sigma_{W^{\pm}+b\bar{b}} = \frac{N'_{W^{\pm}+b\bar{b}}}{\epsilon \cdot \mathcal{A} \cdot \mathcal{L}} \tag{2}$$

We use efficiency, ϵ, and acceptance, $\mathcal{A}$, terms derived from an admixture of data and MC to correct the observed number of $W^{\pm}+b\bar{b}$ events in the 1 and 2 jet bins of the pretag data ($N'_{W^{\pm}+b\bar{b}}$) back to the true number that should have been present in the integrated luminosity of the data ($N_{W^{\pm}+b\bar{b}}$).

The details of the cross-section denominator calculation are described in detail in [3]. Due to the manner in which our $W^{\pm}+b\bar{b}$ MC samples are generated for a specific leptonic decay of the $W^{\pm}$, we chose to change the meaning of our cross-section to be that of a cross-section times branching ratio. To summarize the results of [3], the $W^{\pm}+b\bar{b}$ cross-section in full detail is written as:

$$\sigma_{W^{\pm}+b\bar{b}} \times \mathrm{BR}(W^{\pm} \to \ell\nu) = \frac{N'_{W^{\pm}+b\bar{b}}}{\epsilon_{\mathrm{common}} \sum_{\mathrm{trig}} \left[\epsilon \cdot f_{\mathrm{lep.id}} \cdot \mathcal{L} \cdot \sum_{\mathrm{i}=0}^{2} \left(w_{\mathrm{i}} \cdot \mathcal{A}_{\mathrm{W^{\pm}+b\bar{b}+i}} \right) \right]_{\mathrm{trig}}} \tag{3}$$

where the full denominator has been calculated to be 134.4±15.0(sys.)±8.1(lum.)pb. The numerator of Eq. 3, $N'_{W^{\pm}+b\bar{b}}$, is the number of $W^{\pm}+b\bar{b}$ events in the 1+2 jet bins of the pretag data. We will details its calculation in Sections 4, 5, and 6. For now we note that it comes from fits of the SECVTX mass of tagged jets in our data sample and also from estimates of the b-tag-multiplicity of $W^{\pm}+b\bar{b}$. We can write it as:

$$N'_{W^{\pm}+b\bar{b}} = \frac{n_{\mathrm{fit}} - n_{\mathrm{bkgd.}}}{\kappa_{W^{\pm}+b\bar{b}}} \tag{4}$$

In Eq. 4 n_{fit} is the number of b-jets returned by our fit of the SECVTX mass in tagged events in the 1+2 jet bins, and $n_{\mathrm{bkgd.}}$ is the number of tagged b-jets in the 1+2 jet bins that do not come from $W^{\pm}+b\bar{b}$. $n_{\mathrm{bkgd.}}$ receives contributions from two sources:

$$n_{\mathrm{bkgd.}} = n_{\mathrm{QCD}} + \sum_{MC} n_{\mathrm{MC.}} \tag{5}$$

where n_{QCD} is the number of tagged b-jets from QCD in the 1+2 jet bins, and n_{MC} is the number of tagged b-jets from processes that we use MC to account for. Finally, $\kappa_{W^{\pm}+b\bar{b}}$ is the average number of tagged b-jets in a typical $W^{\pm}+b\bar{b}$ event that has passed all selection through the Pretag stage and ended up in the 1 or 2 jet bins.

2 Theoretical Prediction

To obtain the theoretical prediction for the inclusive $W^{\pm}+b\bar{b}$ cross-section we rely on the Alpgen generator[4]. This program calculates the leading-order (LO) diagrams for $W^{\pm}+b\bar{b}$ production and allows for the treatment of the b-quarks as massive particles[5]. This is important since treating the b-quarks as massless particles introduces divergences in the theoretical $W^{\pm}+b\bar{b}$ cross-section if they are allowed to become arbitrarily collinear. We employ the cuts listed in Table 1 when generating samples. At least one of the b-quarks in the event must pass the cuts shown in Table 1, or if both fail then the combined $b\bar{b}$ pair must fall within a cone of $\Delta\mathrm{R}\leq 0.4$ and pass the cuts. This allows for

events with asymmetric b-quark production, in which one/both of the b-quarks is too soft or down the beampipe, that can contribute to our data to be included in the MC samples.

Parameter	Value
Lepton: η_{max}	5.0
Lepton: p_T min.	1.0 GeV
ΔR(lepton,partons)	1.0
Neutrino: p_T min.	1.0 GeV
Light Partons: η_{max}	3.0
Light Partons: p_T min.	15.0 GeV
Light Partons: ΔR	0.4
Heavy Flavor: η_{max}	3.0
Heavy Flavor: p_T min.	8.0
Heavy Flavor: ΔR	0.0
Heavy Flavor: b-mass	4.7
Q^2	$M_W^2 + \sum m_T^2$

Table 1: Alpgen generator parameters used to make Alpgen v2.1 $W^{\pm} + b\bar{b}$ samples.

We use the Alpgen v2.1 generator to make $W^{\pm}$+$b\bar{b}$+0p, $W^{\pm}$+$b\bar{b}$+1p, and $W^{\pm}$+$b\bar{b}$+2p samples, listed in Table 2, each of which produces a cross-section value. To obtain the final value for the theoretical prediction we sum the generator-level cross-sections of all parton multiplicity samples. There is a large uncertainty in the theoretical predication due to the choice of Q^2 that is used to evaluate the initial matrix-elements that Alpgen generates. The larger the value of Q^2 the smaller the coupling between the initial partons in the collision, which reduces the cross-sections obtained in Alpgen. Conversely, smaller Q^2 values imply larger coupling between the initial partons, which increases the cross-sections obtained in Alpgen.

Table 2 lists "Before MLM" and "After MLM" cross-sections, which refer to the generator-level cross-sections before and after the MLM matching routine has been applied. The matching routine and its effect on our results are discussed in more detail in [3]. We use the cross-section values after the matching has been applied as our final values since they can be added together unambiguously. Table 3 lists the combined cross-sections for the different Q^2 samples. We use the samples generated at $Q^2 = M_W^2 + \sum m_T^2$ as our central values for the theoretical prediction since these are also the samples we used to calculate the central values of our acceptance values (which define the meaning of our experimentally measured value). The uncertainty quoted on the theory value is due to the spread in cross-sections of the different Q^2 samples.

Process	Fileset	Alpgen Version	Generator σ (pb)		Q^2	$N_{\rm gen}$
			Before MLM	After MLM		
$W^{\pm}(\rightarrow e\nu) + b\bar{b}$+0p	etop0x	2.1	2.947±0.064	2.715±0.071	$M_W^2 + \sum m_T^2$	609133
$W^{\pm}(\rightarrow e\nu) + b\bar{b}$+1p	etop1x	2.1	1.354±0.012	0.827±0.015	$M_W^2 + \sum m_T^2$	626365
$W^{\pm}(\rightarrow e\nu) + b\bar{b}$+2p	etop2x	2.1	0.497±0.074	0.283±0.012	$M_W^2 + \sum m_T^2$	618471
$W^{\pm}(\rightarrow e\nu) + b\bar{b}$+0p	xtop0x	2.1	2.385±0.063	2.190±0.064	$4M_W^2$	126830
$W^{\pm}(\rightarrow e\nu) + b\bar{b}$+1p	xtop1x	2.1	1.099±0.011	0.671±0.011	$4M_W^2$	129813
$W^{\pm}(\rightarrow e\nu) + b\bar{b}$+2p	xtop2x	2.1	0.416±0.008	0.239±0.011	$4M_W^2$	128775
$W^{\pm}(\rightarrow e\nu) + b\bar{b}$+0p	xtop3x	2.1	3.043±0.078	2.796±0.086	M_W^2	129813
$W^{\pm}(\rightarrow e\nu) + b\bar{b}$+1p	xtop4x	2.1	1.478±0.014	0.907±0.015	M_W^2	129813
$W^{\pm}(\rightarrow e\nu) + b\bar{b}$+2p	xtop5x	2.1	0.577±0.010	0.336±0.015	M_W^2	129457
$W^{\pm}(\rightarrow e\nu) + b\bar{b}$+0p	xtop6x	2.1	3.978±0.110	3.699±0.110	$\frac{1}{4}M_W^2$	128607
$W^{\pm}(\rightarrow e\nu) + b\bar{b}$+1p	xtop7x	2.1	2.053 ±0.021	1.294± 0.021	$\frac{1}{4}M_W^2$	129240
$W^{\pm}(\rightarrow e\nu) + b\bar{b}$+2p	xtop8x	2.1	0.835±0.014	0.494±0.018	$\frac{1}{4}M_W^2$	128255
$W^{\pm}(\rightarrow \mu\nu) + b\bar{b}$+0p	etop0y	2.1	2.947±0.064	2.714±0.073	$M_W^2 + \sum m_T^2$	622972
$W^{\pm}(\rightarrow \mu\nu) + b\bar{b}$+1p	etop1y	2.1	1.354±0.012	0.827±0.013	$M_W^2 + \sum m_T^2$	612254
$W^{\pm}(\rightarrow \mu\nu) + b\bar{b}$+2p	etop2y	2.1	0.496±0.008	0.284±0.008	$M_W^2 + \sum m_T^2$	573421
$W^{\pm}(\rightarrow \mu\nu) + b\bar{b}$+0p	xtop0y	2.1	2.384±0.061	2.190±0.065	$4M_W^2$	129803
$W^{\pm}(\rightarrow \mu\nu) + b\bar{b}$+1p	xtop1y	2.1	1.099±0.011	0.671±0.012	$4M_W^2$	129708
$W^{\pm}(\rightarrow \mu\nu) + b\bar{b}$+2p	xtop2y	2.1	0.415±0.009	0.240±0.010	$4M_W^2$	128980
$W^{\pm}(\rightarrow \mu\nu) + b\bar{b}$+0p	xtop3y	2.1	3.040±0.075	2.791±0.080	M_W^2	129813
$W^{\pm}(\rightarrow \mu\nu) + b\bar{b}$+1p	xtop4y	2.1	1.479±0.017	0.906±0.022	M_W^2	127522
$W^{\pm}(\rightarrow \mu\nu) + b\bar{b}$+2p	xtop5y	2.1	0.578±0.010	0.338±0.013	M_W^2	129295
$W^{\pm}(\rightarrow \mu\nu) + b\bar{b}$+0p	xtop6y	2.1	3.985±0.105	3.702±0.104	$\frac{1}{4}M_W^2$	129775
$W^{\pm}(\rightarrow \mu\nu) + b\bar{b}$+1p	xtop7y	2.1	2.052±0.019	1.295±0.021	$\frac{1}{4}M_W^2$	129342
$W^{\pm}(\rightarrow \mu\nu) + b\bar{b}$+2p	xtop8y	2.1	0.835±0.016	0.492±0.019	$\frac{1}{4}M_W^2$	116273

Table 2: Alpgen samples used in the study of the effect of Q^2 on $W^{\pm} + b\bar{b}$ cross-section. There is a noticeable trend for decreasing cross-sections as Q^2 is increased that can be attributed to the diminishing value of α_s as Q^2 grows. We sum the "After MLM" cross-sections over all parton multiplicities, for a given Q^2 sample, to come up with the theoretical cross-section value.

3 Data and Event Selection

We use the `bhel0d`, `bhel0h`, `bhmu0d`, and `bhmu0h` datasets which represent all data taken through the summer shutdown of 2005. The data is processed using the 5.3.3_nt version of TopNtuple. The CEM, CMUP, and CMX triggers are relied upon to select high p_T electrons and muons.

Q^2	Electrons: $\sigma_{W^{\pm}+b\bar{b}}$(pb)	Muons: $\sigma_{W^{\pm}+b\bar{b}}$(pb)
$M_W^2 + \sum m_T^2$	3.825±0.074	3.825±0.075
$4M_W^2$	3.100±0.066	3.101±0.067
M_W^2	4.039±0.089	4.035±0.084
$\frac{1}{4}M_W^2$	5.487±0.113	5.489±0.108
Final	3.8±0.9 pb	3.8±0.9 pb

Table 3: Final cross-sections obtained by summing the "After MLM" values over all multiplicitites for the various Q^2 samples in Table 2

We use the v10a of the DQM good run list, with silicon required to be good, to select events. We have removed runs 164844, 194862, and 194900 from the list due to various issues. The integrated luminosity is 694.8±41.7pb^{-1} for the CEM and CMUP triggers, and 654.2±39.3pb^{-1} for the CMX trigger.

For completeness, we list in Table 4 the selection cuts used when running over MC and data. We have followed the default selection recommended by the Top Properties group so that our results can be directly compared with corresponding Method II results[7].

Following the model of the Top Properties group, we now include all additional lepton types in our definition of the DiLepton veto (BMU,CMIO, CMX failing ρ selection, etc...). We are careful to allow CMX muons in the later run ranges to have stubs in the various parts of the detector (Arches, Keystone, Miniskirt) that became functional at different times. We use the jetCorr05b version of the JetUser package to correct jets to level 4, and to estimate systematic uncertainties due to jet energy.

Table 5 summarizes the number of pretag, ≥1 tag, and ≥2 tag events in the combined `bhel0d`, `bhmu0d`, `bhel0h`, and `bhmu0h` data samples. In the 1 and 2 jet bins there are 1541 tagged jets which we will use in our fits of SECVTX mass.

4 MC Templates

We construct templates of the SECVTX mass of different quark flavors (bottom, charm, and light) using tagged jets in various MC samples. We match bottom and charm hadrons in the event shower to tagged jets in the 1 and 2 jet bins by requiring them to be within a cone of $\Delta R \leq 0.4$. If a jet is matched to both a bottom and charm hadron, then we include it in the shape for b-jets. For light-flavor we match light-flavor quarks (u,d,s) in the matrix-element to tagged jets in the 1 and 2 jet bins. We do not allow these light-flavor quarks to be matched to jets that have already been matched to charm or bottom hadrons. We also use negatively tagged jets from the 1 and 2 jet bins of the data as another model of light-flavor tags.

We construct templates in a wide variety of MC samples, listed in Table 6, and

Selection	Cut		
-	Electron	Muon	
		CMUP	CMX
Isolation	<0.1	<0.1	
Region	=0	-	
Fiducial	=1	-	
E_T	≥20.0 GeV	-	
p_T	≥10.0 GeV	≥20.0 GeV	
p_T && E_T	!(<50.0 && ≥100.0)	-	
Had/EM	≤(0.055 + 0.00045· E)	-	
Had	-	≤max(6.0,6.0+0.0280·(p-100.0))	
EM	-	≤max(2.0,2.0+0.0115·(p-100.0))	
E/P && E_T	!(≥2.0 && <100.0)	-	
Δx · Charge	≥-3.0 && ≤1.5	-	
$\|\Delta z\|$	≤3.0 cm	-	
χ^2	StripChi2 ≤10.0	TrkRedChi2CT ≤2.75 (run<190697), ≤2.3 (run≥190697)	
Track L_{shr}	≤0.2	-	
Track Axial Seg.	≥3	≥3	
Track Stereo Seg.	≥2	≥2	
$\|z_0\|$	<60.0 cm	<60.0 cm	
Conversion	false	-	
D0 && Track Si Hits	-	!(≥0.2 && =0) && !(≥0.02 && ≠0)	
CMU $\|\Delta x\|$		<3.0	
CMU Fiducial x		<0.0	
CMU Fiducial z		<0.0	
CMP $\|\Delta x\|$		<5.0	
CMP Fiducial x		<0.0	
CMP Fiducial z		<-3.0	
Bluebeam		false (run<15449)	-
CMX $\|\Delta x\|$			< 6.0
CMX Fiducial x			<0.0
CMX Fiducial z			<-3.0
CMX ρ			<140.0 cm
Arches			
Keystone			
Miniskirt			
Jet E_T	≥15.0 GeV		
Jet Correction Level	Level 4 (jetCorr05b)		
Jet $\|\eta_{\text{detector}}\|$	≤2.0		
GoodRun (w/wo Silicon)	true		
OBSV ($\|z_0\|$)	≤60.0 cm		
≥1 Lepton Candidate	true		
$\not\!\!E_T$	≥20.0 GeV		
Lepton Isol. ≤0.1	true		
DiLepton	false		
Z-veto	false		
$\|z_0 - \text{lepton}z_0\|$	≤5.0 cm		
QCD veto	Not Used		
GoodRun w/ Silicon	true		

Table 4: Cuts used in this analysis to select events through the pretag stage.

then combine these into one final template for each quark flavor. After applying the selection described in Section 3, we normalize the templates from each MC sample by multiplying by the generator-level cross-section and dividing by the number of generated events. This is equivalent to normalizing to the expected shape in 1 pb^{-1}.

-	1 Jet	2 Jet
Pretag		
CEM	39075	6245
CMUP	18059	2748
CMX	9471	1390
$\geq$1 Tag		
CEM	572	300
CMUP	271	143
CMX	161	65
$\geq$2 Tags		
CEM	-	17
CMUP	-	11
CMX	-	1

Table 5: Number of pretag, $\geq$1 tag, and $\geq$2 tag events in the 1 and jets bins of the `0d` and `0h` data sample.

Though we will ultimately let the normalization of each flavor float in our fits, the final templates should represent the shape of bottom, charm, and light found in our data sample since we have tried to include contributions from all relevant processes in the ratios that they actually occur.

The final templates are displayed in Figure 2. We note that the charm template has several peaks in its SECVTX mass distribution that are due to different D-meson resonances, and not due to limited MC statistics.

5 SECVTX Mass Fitting Procedure

The final templates of the SECVTX mass of the different flavors are used to fit for the b-fraction of tagged jets in the 1 and 2 jet bins of the lepton+jets data sample. A binned histogram fit is performed for two different models of the non-b component of the data. In one model negatively tagged jets from the data are used to represent light-flavor jets, while in the other model light-flavor jets from the MC are used. In both cases we apply a Gaussian constraint to the light-flavor component in the fit. The constraint is the predicted number of mistag events in the 1+2 jet bins of the data divided by the total number of tags in those bins, which is 26.3$\pm$4.0%[7].

Figure 3 shows the fit to the 1541 tagged jets in the 1+2 jet bins of the data using two different models of the non-b component. The two fits give similar results, though clearly the different modeling of the light-flavor tags is causing some differences. The fit using negatively tagged jets from the data seems to be doing a slightly better job

Process	Fileset	Cross-Section (pb)
$W^{\pm}(\rightarrow e\nu) + b\bar{b}$+0p	etop0x	2.715
$W^{\pm}(\rightarrow e\nu) + b\bar{b}$+0p	etop1x	0.827
$W^{\pm}(\rightarrow e\nu) + b\bar{b}$+0p	etop2x	0.283
$W^{\pm}(\rightarrow \mu\nu) + b\bar{b}$+0p	etop0y	2.714
$W^{\pm}(\rightarrow \mu\nu) + b\bar{b}$+1p	etop1y	0.827
$W^{\pm}(\rightarrow \mu\nu) + b\bar{b}$+2p	etop2y	0.284
$W^{\pm}(\rightarrow e\nu) + c\bar{c}$+0p	ltop0c	2.453
$W^{\pm}(\rightarrow e\nu) + c\bar{c}$+1p	ltop1c	1.221
$W^{\pm}(\rightarrow e\nu) + c\bar{c}$+2p	ltop2c	0.550
$W^{\pm}(\rightarrow \mu\nu) + c\bar{c}$+0p	ltop3c	2.509
$W^{\pm}(\rightarrow \mu\nu) + c\bar{c}$+1p	ltop4c	1.221
$W^{\pm}(\rightarrow \mu\nu) + c\bar{c}$+2p	ltop5c	0.550
$W^{\pm}(\rightarrow e\nu) + c$+0p	ltop0a	10.767
$W^{\pm}(\rightarrow e\nu) + c$+1p	ltop1a	4.447
$W^{\pm}(\rightarrow e\nu) + c$+2p	ltop2a	1.429
$W^{\pm}(\rightarrow e\nu) + c$+3p	ltop3a	0.436
$W^{\pm}(\rightarrow \mu\nu) + c$+0p	ltop4a	10.748
$W^{\pm}(\rightarrow \mu\nu) + c$+1p	ltop5a	4.447
$W^{\pm}(\rightarrow \mu\nu) + c$+2p	ltop6a	1.429
$W^{\pm}(\rightarrow \mu\nu) + c$+3p	ltop7a	0.475
$W^{\pm}(\rightarrow e\nu)$+1p	ltop1n	436.8
$W^{\pm}(\rightarrow e\nu)$+2p	ltop2n	99.0
$W^{\pm}(\rightarrow e\nu)$+3p	ltop3n	22.7
$W^{\pm}(\rightarrow e\nu)$+4p	ltop4n	5.2
$W^{\pm}(\rightarrow \mu\nu)$+1p	ltop1m	436.8
$W^{\pm}(\rightarrow \mu\nu)$+2p	ltop2m	99.0
$W^{\pm}(\rightarrow \mu\nu)$+3p	ltop3m	22.7
$W^{\pm}(\rightarrow \mu\nu)$+4p	ltop4m	5.2
$t\bar{t}$	ttopkl	6.7
Single-Top (s-chan.)	mtopya	0.88
Single-Top (t-chan.)	mtopta + ua_match	1.98
$W^{\pm}W^{\pm}$	wtop1w	12.4

Table 6: MC samples used in construction of SECVTX mass templates.

of modeling the shape of the data, so we will use that as our central value and quote a systematic on our results due to the differences seen when using light-flavor MC. The b-fraction of 26.4% obtained in the fit using negatively tagged jets as a model for light-flavor corresponds to $406.1 \pm^{47.1}_{45.3}$ tagged b-jets. Table 7 summarizes the fit results

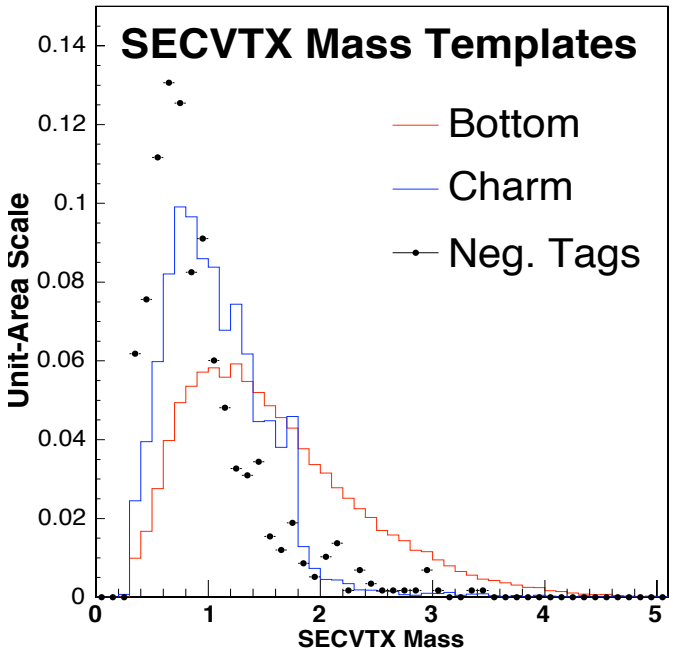

Figure 2: Templates of SECVTX mass for bottom, charm, and negative tags in the data.

in the 1, 2, and 1+2 jet bins for the two non-b models.

Figure 4 shows the SECVTX mass fits in the individual 1 and 2 jet bins, using negative jets as the model for light-flavor. The charm fraction is much larger in the 1-jet bin than in the 2-jet bin, which is presumably due to the presence of $W^{\pm}c$ in the 1-jet bin.

Component	1 jet	2 jet	1+2 jets
Bottom	$18.78 \pm {}^{3.57}_{3.36}$	$39.66 \pm {}^{5.64}_{5.28}$	$26.35 \pm {}^{3.05}_{2.93}$
Charm	$54.66 \pm {}^{3.36}_{4.99}$	$39.57 \pm {}^{6.65}_{6.64}$	$47.2 \pm {}^{4.43}_{4.40}$
Neg. Tags	$26.71 \pm {}^{3.22}_{3.2}$	$21.32 \pm {}^{3.26}_{3.26}$	$26.42 \pm {}^{3.01}_{3.01}$
Bottom	$22.11 \pm {}^{3.59}_{3.4}$	$41.81 \pm {}^{5.86}_{5.49}$	$28.89 \pm {}^{3.09}_{2.96}$
Charm	$52.02 \pm {}^{5.07}_{5.05}$	$39.53 \pm {}^{6.72}_{6.74}$	$49.09 \pm {}^{4.28}_{4.32}$
Light	$26.1 \pm {}^{3.06}_{3.04}$	$19.65 \pm {}^{3.11}_{3.10}$	$22.36 \pm {}^{2.68}_{2.64}$
Mistag Constraint	27.8±4.2	23.2±3.6	26.3±4.0

Table 7: Results of SECVTX mass fit in 1,2, and 1+2 jet bins of data for two different models of the non-b component. All numbers are %.

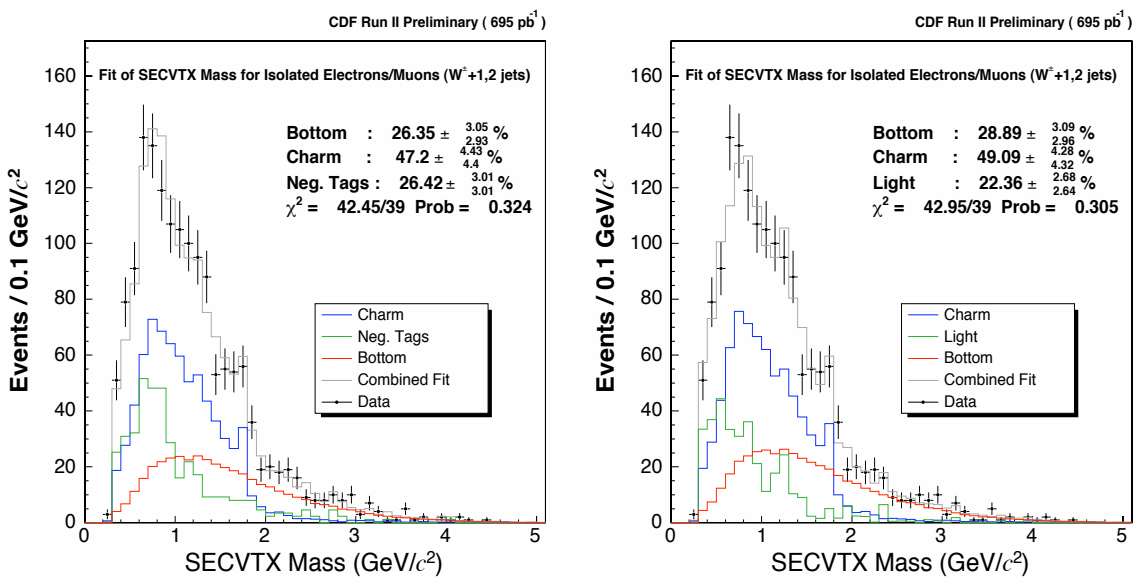

Figure 3: Fit of the SECVTX Mass of tagged jets in our signal region. Left: This fit used charm and negative tags as the model for "non-b". Right: This fit uses charm and light-flavor from MC as the model for "non-b".

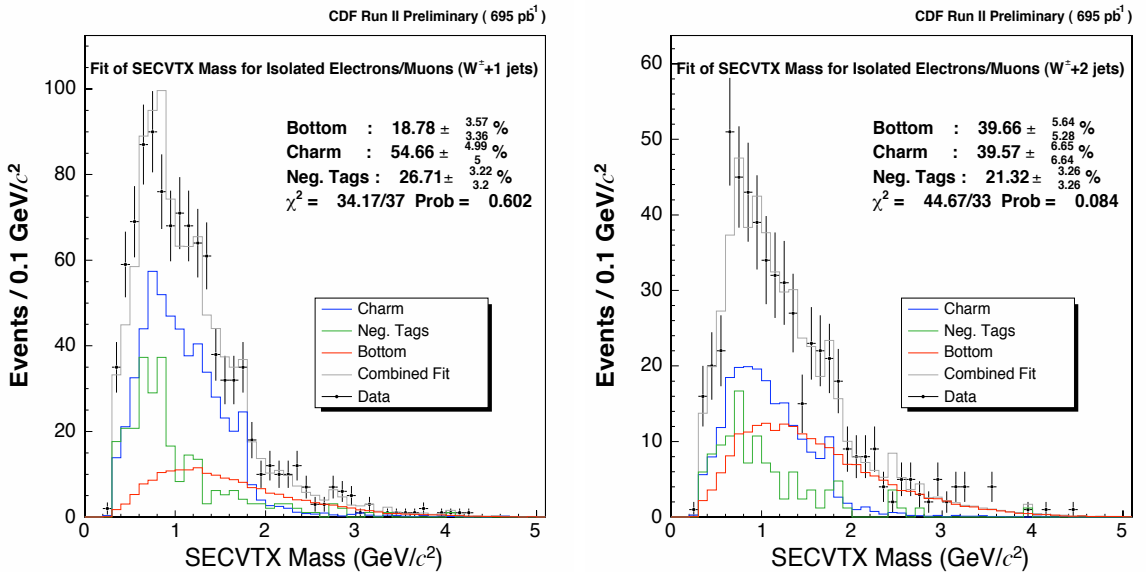

Figure 4: Fit of the SECVTX Mass of tagged jets in the 1 (Left) and 2 (Right) jet bins separately. Both fits use negative tags as the model for light-flavor.

6 Background b-jet Sources

There are two main components of the number of background b-jets in the 1+2 jet bins of the data:

1. $n_{\rm QCD}$: tagged b-jets from QCD, which we will calculate using data
2. $n_{\rm MC}$: tagged b-jets from processes that we must use MC to calculate.
   - $t\bar{t}$
   - Single-Top (s-channel and t-channel)
   - DiBoson - WZ/WW/ZZ
   - $W^{\pm}(\rightarrow \tau\nu) + b\bar{b}$+N partons
   - $Z \rightarrow \tau\tau$
   - $Z + b\bar{b}$

6.1 $n_{\rm QCD}$

To estimate the number of tagged b-jets in the 1+2 jet bins coming from QCD, we multiply the expected number of QCD events in the signal region, $N_{\rm QCD}$, (which we get using the $\not\!\!E_T$ vs. Isol. method) by the b-fraction of anti-isolated events, f_b, (which we get from a SECVTX mass fit) as shown in Eq. 6. We treat electrons and muons separately since they have different b-fractions in the anti-isolated samples. Table 8 lists the estimates of $N_{\rm QCD}$ from the Method II analysis for the current data sample[7].

$$n_{\rm QCD} = (f_b \cdot N_{\rm QCD})_{\rm electrons} + (f_b \cdot N_{\rm QCD})_{\rm muons} \tag{6}$$

Method	`0d` data		`0h` data	
	1-jet	2-jet	1-jet	2-jet
Electrons				
Tag-Rate	30.35±7.67	15.14±3.95	39.01±9.85	17.11±4.45
$\not\!\!E_T$ vs. Isol	50.97±4.54	23.39±3.12	76.59±5.62	24.54±3.06
Muons				
Tag-Rate	8.16±2.12	4.71±1.32	10.87±2.81	3.84±1.10
$\not\!\!E_T$ vs. Isol.	8.41±1.09	4.66±0.93	15.01±1.57	4.55±0.91

Table 8: Estimates of tagged QCD events in the signal region from two different methods. A weighted average of the two methods is taken, after first combining electrons and muons, to obtain the final QCD event estimate.

Figure 5 shows the SECVTX mass fit in two different regions of the non-isolated data ($\not\!\!E_T$ $\leq$15.0 GeV, $\not\!\!E_T$ $\geq$20.0 GeV) for electrons and muons. The $\not\!\!E_T$ $\leq$15.0 GeV region has large statistics and the resulting fits agree well with the data. The $\not\!\!E_T$ $\geq$20.0 GeV region has much smaller statistics but returns very similar, albeit much less sensitive, b-fractions.

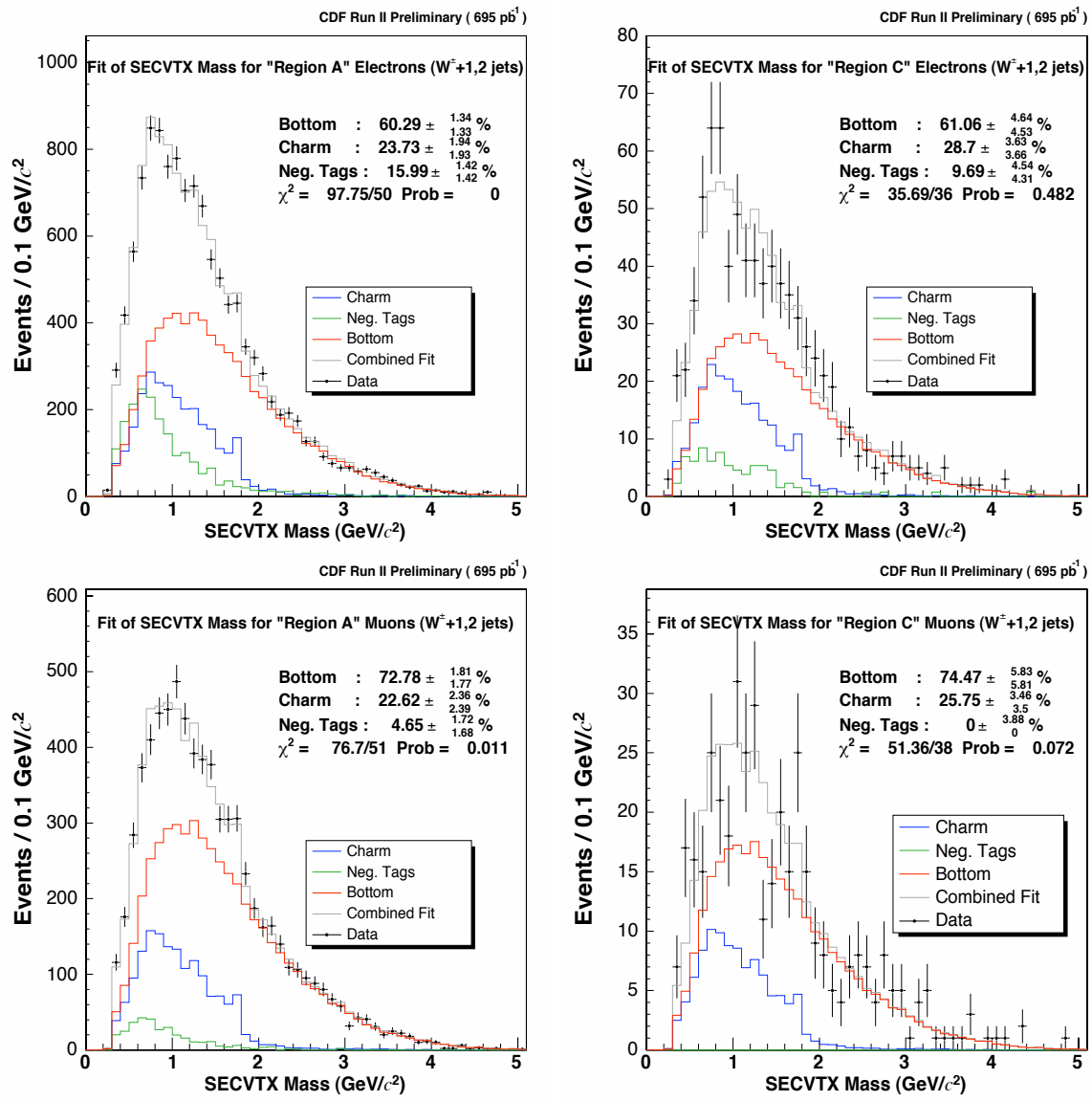

Figure 5: SECVTX Mass fits of tagged jets in different regions of the $\not\!\!E_T$ vs. Isolation plane.

We apply the resulting b-fractions from the non-isolated $\not\!\!E_T$ $\geq$20.0 GeV region to

estimates of the number of QCD events that come from both the $\not\!\!E_T$ vs. Isolation method and the "Tag-Rate" method. After taking the weighted average for the two methods we obtain 91.17±18.47 tagged b-jets from QCD in the 1+2 jet bins. The uncertainty quoted is due to the uncertainty of the event estimates of Table 8 and also due to the uncertainty of the b-fraction obtained in the non-isolated SECVTX mass fits. We describe additional systematics later in the note.

6.2 n_{MC}

To estimate the number of tagged b-jets in the 1+2 jet bins coming from the remaining backgrounds mentioned above, we rely strictly on the MC for each process. We apply the standard selection to these samples, and count how many events are in the 1 or 2 jet bins of the pretag data and have at least one b-jet (a jet matched to a b-hadron via a ΔR cone of 0.4). For these events we then count how many tagged b-jets appear in the final sample. Eq. 7 represents the calculation of the number of background b-jets for a given process:

$$n_{\mathrm{MC}} = \sigma_{MC} \cdot \mathcal{L} \cdot \sum_{i=1}^{2} \Big(f_{1b} \cdot \epsilon_{tag1b} \cdot \mathrm{SF} + f_{2b} \cdot (\epsilon_{tag2b} \cdot \mathrm{SF} + 2 \cdot \epsilon_{2tag2b} \cdot \mathrm{SF}^2) \Big)_i \qquad (7)$$

In Eq. 7 the following terms are used:

- σ_{MC}: Cross-section of process.
- $\mathcal{L}$: Luminosity we wish to scale to.
- f_{1b}: Fraction of initial events that pass selection and have one identified b-jet
- f_{2b}: Fraction of initial events that pass selection and have two identified b-jets
- ϵ_{tag1b}: Fraction of $1b$ events in which the b-jet is tagged.
- ϵ_{tag2b}: Fraction of $2b$ events in which one of the b-jets is tagged.
- ϵ_{2tag2b}: Fraction of $2b$ events in which both of the b-jets are tagged.
- SF: b-tag scale factor, 0.89±0.07[8].

In Eq. 7 we are just summing over the 1 and 2 jet bins of each MC process to get the number of tagged b-jets the process will contribute in the given luminosity. Clearly, for the 1-jet bin the contributions of the $2b$ category will be zero. This is essentially the procedure followed to estimate the W+HF process in the Method II analysis, but here we are adding up b-jets instead of events (hence the factor of "2" in front of the ϵ_{2tag2b} term).

We apply this procedure to the MC samples listed in Table 9, which yields the results in Table 10. To obtain the numbers in Table 9 we have separated out all the calculations of Eq. 7 by trigger type (CEM, CMUP, CMX) to account for any differences in heavy-flavor fraction, tagging efficiencies, luminosities.

Process	Cross-Section (pb)	Fileset	Events
$W^{\pm}(\rightarrow \tau\nu) + b\bar{b}$+0p	2.715±0.071	`atop0t`	250966
$W^{\pm}(\rightarrow \tau\nu) + b\bar{b}$+2p	0.283±0.012	`atop2t`	244986
$W^{\pm}W^{\pm}$	12.4±0.25	`wtop1w`	419728
$W^{\pm}Z$	3.96±0.06	`wtop1z`	409647
ZZ	1.58±0.02	`ztopcz`	412866
Single-top (s-channel)	0.88±0.05	`mtopya`	195928
Single-top (t-channel)	1.98±0.08	`mtopta` + `ua_match`	144525
$Z(\rightarrow \ell^{+}\ell^{-}) + b\bar{b}$+0p	0.5376±0.0008	`ztop0b`	148608
$Z(\rightarrow \tau\tau)$	252.0±9.0	`ztop1i`	925632
$t\bar{t}$	6.7±0.7	`ttopkl`	1846011

Table 9: Summary of MC sources and information needed to calculate background b-jet contributions from each. We assumed the cross-sections of $W^{\pm}(\rightarrow \tau\nu) + b\bar{b}$ to be the same as the electron/muon MC we have for that process, since the actual cross-section for that MC is missing. We only have $Z + b\bar{b}$ MC for the electron channel, so the results obtained in that sample are doubled to account for any contributions from the muon channel.

Process	1-jet	2-jet	1+2 jets
$W^{\pm}(\rightarrow \tau\nu) + b\bar{b}$+0p	2.93 ± 0.20	1.69 ± 0.17	4.63 ± 0.27
$W^{\pm}(\rightarrow \tau\nu) + b\bar{b}$+2p	0.23 ± 0.02	0.49 ± 0.03	0.73 ± 0.04
$W^{\pm}W^{\pm}$	0.14 ± 0.08	0.63 ± 0.16	0.77 ± 0.17
$W^{\pm}Z$	2.39 ± 0.17	4.98 ± 0.28	7.37 ± 0.33
ZZ	0.06 ± 0.02	0.25 ± 0.04	0.31 ± 0.04
Single-top (s-channel)	4.22 ± 0.18	15.42 ± 0.61	19.64 ± 0.64
Single-top (t-channel)	14.18 ± 0.48	15.24 ± 0.51	29.42 ± 0.70
$Z(\rightarrow \ell^{+}\ell^{-}) + b\bar{b}$+0p	2.44 ± 0.15	3.26 ± 0.19	5.70 ± 0.24
$Z(\rightarrow \tau\tau)$	1.53 ± 0.77	0.76 ± 0.59	2.29 ± 0.97
$t\bar{t}$	6.20 ± 0.46	52.10 ± 3.58	58.30 ± 3.61
Total	34.32 ± 1.08	94.83 ± 3.74	129.15 ± 3.89

Table 10: Summary of tagged b-jets from MC sources. Uncertainties shown are those due to MC statistics and generator-level cross-section.

Source	1-jet	2-jet	1+2 jets
MC Stat./$\sigma_{\rm MC}$	1.08	3.74	3.89
Scale Factor	2.70	9.33	12.03
Lum.	2.06	5.69	7.75
Total	34.32 ± 3.56	94.83±11.55	129.15±14.83

Table 11: Summary of uncertainties on the estimate of the number of tagged b-jets from various MC sources. The dominant uncertainty is due to the b-tag scale factor, followed by the 6% uncertainty of the luminosity.

There will be systematic uncertainty on these background estimates due to the uncertainty of the b-tag scale-factor, the 6% uncertainty of the luminosity, and the inherent uncertainty of the calculation (due to MC statistics and cross-section uncertainties). Table 11 summarizes the various sources of uncertainty in the calculation of the number of background b-jets. We have treated the scale-factor uncertainty as being correlated across trigger channels and jet bins, and similarly treated the luminosity uncertainty.

7 $W^{\pm}+b\bar{b}$ Tag-Multiplicity: $\kappa_{W^{\pm}+b\bar{b}}$

The final piece needed to finish the cross-section is an estimate of the average number of tagged b-jets in a $W^{\pm}+b\bar{b}$ event in the pretag data, which we call $\kappa_{W^{\pm}+b\bar{b}}$. This is calculated by first counting the number of $W^{\pm}+b\bar{b}$ events in all the $W^{\pm}+b\bar{b}$+Np MC that pass selection and make it into each jet bin of the pretag data ($N_{W^{\pm}+b\bar{b}}$). We then count the number of tagged b-jets that come from each of these events. Dividing the number of tagged b-jets by the number of events gives us the value of $\kappa_{W^{\pm}+b\bar{b}}$ for each $W^{\pm}+b\bar{b}$+Np sample. Eq. 8 is used to calculate $\kappa_{W^{\pm}+b\bar{b}}$ in a given jet bin:

$$\kappa_{W^{\pm}+b\bar{b}}(i^{th}\text{ bin}) = \left(\frac{N''_{W^{\pm}+b\bar{b}\ 1b} \cdot SF + N''_{W^{\pm}+b\bar{b}\ 2b} \cdot SF + 2 \cdot N''_{W^{\pm}+b\bar{b}\ 2-2b} \cdot SF^2}{N_{W^{\pm}+b\bar{b}}} \right)_i \quad (8)$$

In Eq. 8 $N''_{W^{\pm}+b\bar{b}\ 1b}$ is the number of $W^{\pm}+b\bar{b}$ events in the i^{th} jet bin with 1 identified b-jet that is tagged, $N''_{W^{\pm}+b\bar{b}\ 2b}$ ($N''_{W^{\pm}+b\bar{b}\ 2-2b}$) is the number of events in the i^{th} jet bin with 2 identified b-jets and one (two) of them tagged.

The following tables show those calculations for the 1 (Table 12) and 2 (Table 13) jet bins, as well as for the combined 1+2 jet bins (Table 14). The final value of $\kappa_{W^{\pm}+b\bar{b}}$ is calculated via a weighted sum of the individual $W^{\pm}+b\bar{b}$+Np samples (Table 15), where the weight is the cross-section for a given sample divided by the total cross-section of all samples.

	$We\nu b\bar{b}0p$	$We\nu b\bar{b}1p$	$We\nu b\bar{b}2p$	$W\mu\nu b\bar{b}0p$	$W\mu\nu b\bar{b}1p$	$W\mu\nu b\bar{b}2p$
$N_{W^{\pm}+b\bar{b}}$	43134	79793	40663	36394	63685	31281
$N''_{W^{\pm}+b\bar{b}\ 1b}$	15510	7598	2183	13020	6102	1660
$\kappa_{W^{\pm}+b\bar{b}}$	0.320±0.003	0.085±0.001	0.048±0.001	0.318±0.004	0.085±0.001	0.047±0.001

Table 12: Tag-multiplicity numbers for the 1-jet bin of different $W^{\pm}+b\bar{b}$ MC. The uncertainty values are those due to the MC statistics only.

	$We\nu b\bar{b}0p$	$We\nu b\bar{b}1p$	$We\nu b\bar{b}2p$	$W\mu\nu b\bar{b}0p$	$W\mu\nu b\bar{b}1p$	$W\mu\nu b\bar{b}2p$
$N_{W^{\pm}+b\bar{b}}$	8604	40297	63670	7361	32800	48725
$N''_{W^{\pm}+b\bar{b}\ 1b}$	537	13800	9745	508	11170	7481
$N''_{W^{\pm}+b\bar{b}\ 2b}$	3283	1910	634	2802	1557	503
$N''_{W^{\pm}+b\bar{b}\ 2-2b}$	1231	638	180	1042	535	142
$\kappa_{W^{\pm}+b\bar{b}}$	0.622±0.013	0.372±0.004	0.150±0.002	0.625±0.015	0.371±0.004	0.150±0.002

Table 13: Tag-multiplicity numbers for the 2-jet bin of different $W^{\pm}+b\bar{b}$ MC. The uncertainty values are those due to the MC statistics only.

	$We\nu b\bar{b}0p$	$We\nu b\bar{b}1p$	$We\nu b\bar{b}2p$	$W\mu\nu b\bar{b}0p$	$W\mu\nu b\bar{b}1p$	$W\mu\nu b\bar{b}2p$
$\kappa_{W^{\pm}+b\bar{b}}$	0.370±0.003	0.181±0.001	0.110±0.001	0.370±0.003	0.183±0.002	0.110±0.001

Table 14: Tag-multiplicity numbers for 1+2-jet bins of different $W^{\pm}+b\bar{b}$ MC. The uncertainty values are those due to the MC statistics only.

It is interesting to observe the trend for $\kappa_{W^{\pm}+b\bar{b}}$ in the combined 1+2 jet bins shown in Table 14. It is clear that the value of $\kappa_{W^{\pm}+b\bar{b}}$ decreases as more partons are added to the matrix-elements. One possible explanation for this trend is that in order for a $W^{\pm}+b\bar{b}$+0p event to fall into the 1 or 2 jet bins at least one of the b-quarks must be fairly central to the detector, whereas for the $W^{\pm}+b\bar{b}$+2p events to fall into the 1 or 2 jet bins the b-quarks need not be central as long as one of the light-flavor partons is. Hence, $W^{\pm}+b\bar{b}$+0p events in the 1or 2 jet bins are more likely to contain tags than $W^{\pm}+b\bar{b}$+2p.

To get the final value of $\kappa_{W^{\pm}+b\bar{b}}$ in the combined 1 and 2 jet bins we do a weighted sum over the different parton multiplicity samples, using the same cross-section weights from the acceptance calculation. The final results are displayed in Table 15 with MC statistics uncertainty only. Table 16 shows the results for the 1+2 jet bins with the uncertainty from the scale-factor calculated.

	1-jet Bin		2-jet Bin		1+2-jet Bin	
	Electrons	Muons	Electrons	Muons	Electrons	Muons
$\kappa_{W^{\pm}+b\bar{b}}$	0.249±0.001	0.248±0.001	0.533±0.001	0.535±0.001	0.310±0.003	0.310±0.004

Table 15: Combined Tag-multiplicity numbers for 1+2-jet bin. The uncertainty values are those due to the MC statistics only.

-	Electrons	Muons
$\kappa_{W^{\pm}+b\bar{b}}$	0.310±0.003(stat.)±0.027(SF)	0.310±0.004(stat.)±0.027(SF)

Table 16: Combined numbers for 1+2-jet bin..

8 Systematic Uncertainties

We have considered many sources of systematic uncertainty for each component of the cross-section calculation. We summarize those sources in this section.

8.1 n_{fit} Systematics

The number of tagged b-jets obtained in our fit of the 1 and 2 jet data has several sources of uncertainty related to the SECVTX mass templates. Since we rely on these templates to separate tagged jets from bottom, charm, and light-flavor we need to determine the impact of any systematic source on the value obtained for the b-fraction.

8.1.1 Dijet Mass Study

In order to determine if our templates of SECVTX mass for b-jets in the MC resembles the distribution of b-jets in the data, we rely on an alternative data sample with very pure b-content. As in the previous $W^{\pm}+b\bar{b}/W^{\pm}+1,2j$ ratio analysis, we smear our templates for b-jets based on differences observed in a study of double-tagged dijet events with one identified semileptonic decay[9]. The "away-jet", which is on the opposite side of the detector as the semileptonic decay jet, was found to have a very high-purity b-fraction (99%). We assumed that any differences in the SECVTX mass shapes of the away-jets in the data and the MC templates used in the dijet fit could be attributed to differences in modeling b-decays in the MC vs. the data. We smear our templates with the ratio of the data and MC shapes from this analysis, shown in Figure 6, and redo our SECVTX mass fits.

As we saw in the previous $W^{\pm}+b\bar{b}/W^{\pm}+1,2j$ ratio analysis, this is a large effect. The b-fraction obtained after smearing is 29.0±3.6%, which amounts to a 10.1% difference in the estimated number of tagged b-jets in the data. Similarly, in our fits of the non-isolated data that are used to estimate QCD, we see the b-fractions increase by

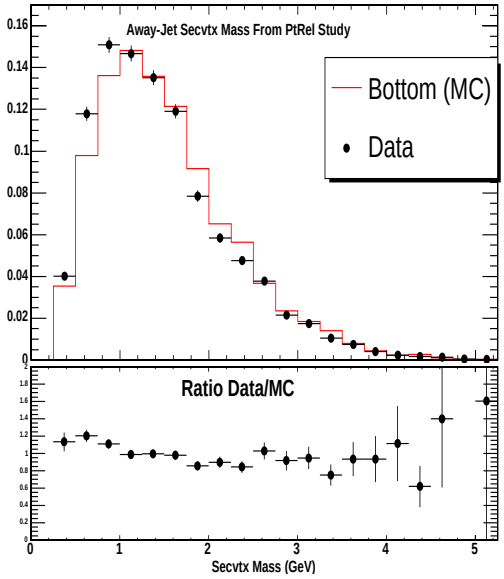

Figure 6: "Away"-jet SECVTX Mass shapes in double-tagged dijet data/MC with one identified semileptonic decay, and tags on opposite sides of the detector. The ratio of Data/MC shown here is used to smear the templates of SECVTX mass derived from Lepton+Jets MC, and the resulting templates are used in our fit to estimate a systematic uncertainty.

approximately 5% (for electrons and muons), which translates into an 8.1% increase in the predicted number of tagged b-jets from QCD.

8.1.2 non-b Model

Earlier we mentioned that different b-fractions were obtained when we used negatively tagged jets to represent light-flavor, versus when we used light-flavor from MC. Table 7 shows that the b-fractions were different by 2.5%. We take half this difference to be our systematic uncertainty caused by our non-b model, which translates into a 4.8% systematic on the number of tagged b-jets. The b-fractions of electrons and muons in our non-isolated fits (for the QCD estimate) both decrease by <1% when we use light MC instead of negative tags. Taking half this difference, as we do for the signal fit, translates into a decrease in of 0.5% in the predicted number of tagged b-jets from QCD.

The templates used to represent light-flavor both suffer from low statistics. Possible improvements could come from either generating more light-flavor MC tags, or parameterizing the shapes with a smooth function.

8.1.3 MC Statistics

The uncertainty returned by our likelihood fitting code is only due to the statistics of the data that we are fitting. We rely on the TFractionFitter program to determine the uncertainty due to the statistics of the MC templates. We estimate this uncertainty in the same manner as was done for the $W^{\pm}+b\bar{b}/W^{\pm}+1,2j$ ratio analysis, in which the statistics of the MC templates are artificially increased by a factor of 10,000 and the the error on the resulting b-fraction is subtracted off the error from the default template fit. The difference is quoted as the systematic uncertainty due to MC statistics:

$$\Delta_{\mathrm{MC}} = \sqrt{\left((Err_{tot}^{fit})^2 - (Err_{10^4}^{fit})^2\right)} \tag{9}$$

Applying this method we find shifts of less than 1% in the uncertainty of the b-fraction obtained when using negative tags as a light-flavor model. This corresponds to a 4.0% uncertainty in the number of tagged b-jets returned by our fit.

8.1.4 Single/Double HF Jet Templates

It is possible that some jets in our templates are actually matched to multiple HF hadrons. If the SECVTX mass shapes of these jets is significantly different than jets that are matched to only one HF hadron, then we would need to determine if our templates had the correct proportions of both types of jet. In our MC templates of bottom and charm jets, the bottom jets are 92% single-b vs. 8% double-b, while the charm jets are 87% single-c vs. 13% double-c. Figure 7 shows the templates for tagged bottom and charm jets that are matched to one or two HF hadrons.

Figure 7 shows that charm jets in particular look different depending on how many HF hadrons they contain. To estimate the systematic uncertainty due to this behavior we fluctuate the proportions of single to double HF jets in our bottom and charm templates. Eq. 10 represents the sum of the number of single (N_1) and double (N_2) HF jets. Our default templates have $x_1 = x_2 = 1$.

$$x_1 \cdot \frac{N_1}{N_1 + N_2} + x_2 \cdot \frac{N_2}{N_1 + N_2} = 1 \tag{10}$$

We keep the integral of our templates constant while changing the relative proportions. We increase the proportion of single HF jets by changing x_1 up to 1.1 and then down to 0.9, and at the same time we must decrease the proportion of double HF jets to $x_2 = 1 + \frac{N_1}{N_2}(1 - x_1)$.

The b-fractions appear relatively stable as we vary the proportions of single and double HF jets in our templates. The biggest change occurs when we increase the fraction of single-charm relative to the double-charm shape. The double-charm shape has a long tail above a SECVTX mass of 2.0 GeV, so by reducing this contribution

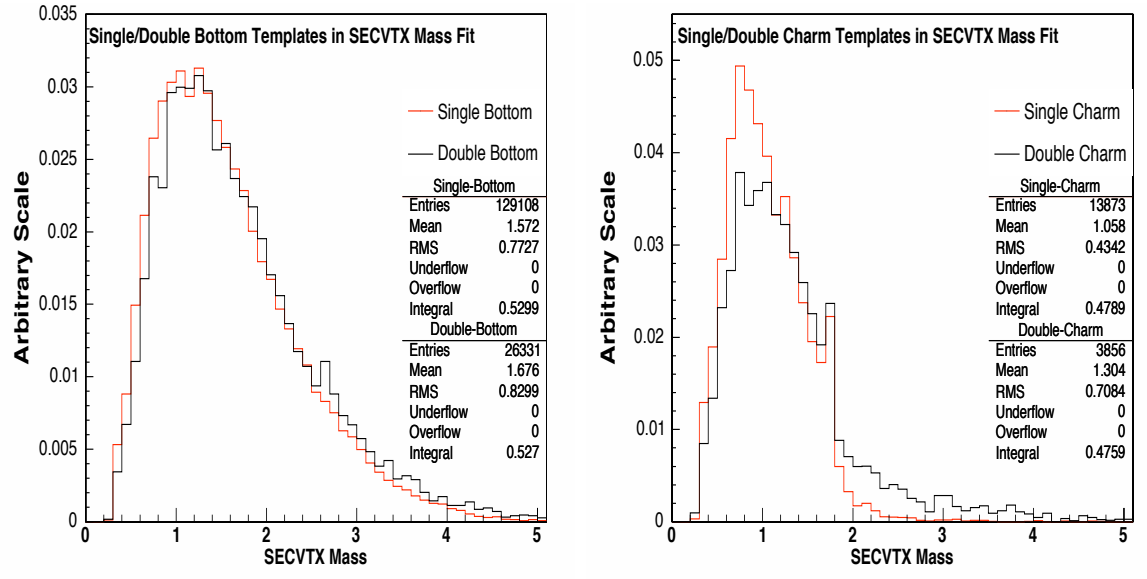

Figure 7: SECVTX mass templates for jets matched to one or two HF hadrons.

Single b (%)	Double b (%)	Single c (%)	Double c (%)	b-fraction (%)
92.0	8.0	87.0	13.0	26.4±3.1
100.0	0.0	87.0	13.0	26.8±3.1
82.9	17.1	87.0	13.0	25.9±3.0
92.0	8.0	95.7	4.3	28.0±3.0
92.0	8.0	78.3	21.7	24.7±3.2

Table 17: b-fraction obtained after varying proportions of single and double HF jets in our templates. The top row represents the default templates.

to the overall charm shape it is not surprising that the b-fraction (which is largely driven by the tail of the data distribution) increases. We quote half of the maximum deviation from the default templates (which occurs when we decrease the double-charm jets) as our systematic. This corresponds to a difference of 0.8% in the b-fraction and a change of 3.0% in the number of tagged b-jets returned by our fit. Varying the single and double HF jet proportions in the QCD fit has a very small effect on the resulting b-fraction, so we assign no systematic to that estimate.

8.2 n_{bkgd} Systematics

We consider systematics on the number of tagged b-jets from QCD and from various MC sources separately.

8.2.1 n_{QCD} Systematics

The only remaining systematic on n_{QCD} that has not been addressed is that due to which region of the $\not\!\!E_T$ vs. Isolation plane we chose to fit to represent QCD. If we fit the $\not\!\!E_T$ $\leq$15.0 GeV and isolation$\leq$0.1 region, instead of the $\not\!\!E_T$ $\geq$20.0GeV and isolation$\geq$0.1 region, the b-fraction comes out much lower (43.6% vs. 61.09% for electrons, 47.4% vs. 74.47% for muons). We take the difference in these two regions to be the systematic for our estimate of the b-fraction of QCD events. This corresponds to a 30.4% uncertainty in the estimated number of b-jets from QCD.

8.2.2 n_{MC} Systematics

The only systematics considered for the estimate of n_{MC} are those due to b-tag scale-factor, luminosity, and MC statistics. The size of each systematic has already been listed in Table 9. The b-tag scale-factor is the largest source of uncertainty in this background estimate, followed by the 6% luminosity uncertainty.

8.3 $\kappa_{W^{\pm}+b\bar{b}}$ Systematics

We have already discussed the systematic uncertainties in the calculation of $\kappa_{W^{\pm}+b\bar{b}}$, as shown in Table 16. The error on the b-tag scale-factor (SF=0.89$\pm$0.07) is treated as a systematic and added in quadrature with uncertainty due to MC statistics. The total uncertainty on $\kappa_{W^{\pm}+b\bar{b}}$ is 8.8%.

8.4 Denominator Systematics

We discuss the calculation of the cross-section denominator in [3]. The numbers needed for the calculation of the denominator, along with their respective uncertainties, are summarized in Table 18. Many sources of systematic uncertainty were considered in the calculation of the acceptance for $W^{\pm}+b\bar{b}$ in each trigger channel, and these are summarized in Table 19.

-	CEM	CMUP	CMX
ϵ_{common} (z_0)	0.9555±0.0004±0.003		
$\epsilon_{trig.}$	0.9755±0.0055	0.9157±0.0031	0.9623±0.0028
f_{id}	0.9810±0.0030	$0.9472\pm^{0.0034}_{0.0043}$	$1.0014\pm^{0.0039}_{0.0178}$
$\mathcal{A}$	0.120±0.013	0.070±0.008	0.030±0.004
$\mathcal{L}$	694.8±41.7 pb^{-1}	694.8±41.7 pb^{-1}	654.2±39.3 pb^{-1}
Denom.	**134.37± 14.97(sys.)± 8.06 (lum.) pb^{-1}**		

Table 18: Final numbers needed for the calculation of the $W^{\pm} + b\bar{b}$ cross-section denominator. The uncertainties quoted on the acceptance numbers are the quadratic sum of all the various categories of systematics considered. In our final calculation of the "Denom." value we treat the different categories of systematic uncertainty (PDF, Jet-Energy, etc...) on the acceptances as being correlated across trigger channels.

Source	Value (%)
Collision Q^2	7.08
Luminosity	6.0
Jet Energy	5.59
PDF	4.62
Shower Q^2	4.5
Herwig/Pythia	1.0
Trig. Efficiencies	0.34
Lepton ID	0.33
z_0 Efficiency	0.31
Total	12.7

Table 19: Final Systematics for the calculation of the $W^{\pm} + b\bar{b}$ cross-section denominator. The Herwig/Pythia systematic is artificially quoted as 1%. We are still estimating this uncertainty and will update it in a subsequent version of this note.

9 Results and Conclusions

The final numbers needed to calculate the $W^{\pm}+b\bar{b}$ cross-section are displayed in Table 20. The final cross-section is found to be 4.46±1.13(stat.)±1.64(syst.)pb. This is to be compared to the theoretical prediction of 3.8±0.9pb. These two values are in agreement, though the large uncertainty of the measured value makes it difficult to draw any stronger conclusions.

Table 21 summarizes the sources of systematic uncertainty on the $W^{\pm}+b\bar{b}$ cross-section. The leading sources of uncertainty in this analysis are those from dijet mass study, and those related to modeling the QCD component of the background. Both of these have potential remedies that may reduce the systematic uncertainty on the cross-section. For the dijet mass systematic we could potentially use the template of SECVTX mass for tagged b-jets in this study as the template for our bottom templates, effectively eliminating this as a source of systematic uncertainty. For the estimation of the number of tagged b-jets from QCD, reducing the uncertainty of the b-fraction of tagged jets from QCD could potentially be achieved with more sophisticated methods of estimating the value of this quantity in the signal region. Parameterizing the "light" shapes (either from neg. tags or from light-flavor MC) with a smooth function could also help reduce some of the systematic uncertainty.

Variable	Value	Stat.	Sys.
n_{fit}	406.1	47.1	49.8
n_{MC}	129.15	-	14.8
n_{QCD}	91.17	-	34.1
$\kappa_{W^{\pm}+b\bar{b}}$	0.310	-	0.027
$\epsilon \cdot \mathcal{A} \cdot \mathcal{L}$ (pb^{-1})	134.37	-	17.0
$\sigma_{W^{\pm}+b\bar{b}}$ (pb)	4.46	1.13	1.64

Table 20: Final numbers needed for the calculation of the $W^{\pm}+b\bar{b}$ cross-section.

While the uncertainties on the measured $W^{\pm}+b\bar{b}$ cross-section are large, the results are encouraging. As mentioned in the preceding paragraph, several of the leading sources of systematic uncertainty may already be on the verge of being reduced. Other potential improvements could come from optimizing our selection cuts to discriminate against QCD while keeping as much of the $W^{\pm}+b\bar{b}$ signal as possible (by either raising the $\not\!\!E_T$ cut or adding in the QCD $\Delta\phi$ cut).

Variable	Source	Value (%)
n_{fit}	Dijet Mass Study	22.1
	non-b Model	10.5
	MC Statistics	8.7
	Double HF	6.6
n_{QCD}	QCD Model	14.9
	MET vs. Isol.	9.9
	Dijet Mass Study	4.0
	non-b Model	0.3
n_{MC}	SF	6.5
	Lum.	4.2
	MC Statistics	2.1
$\kappa_{W^{\pm}+b\bar{b}}$	SF	8.7
	MC Statistics	1.0
Denominator	Collision Q^2	7.08
	Luminosity	6.0
	Jet Energy	5.59
	PDF	4.62
	Shower Q^2	4.5
	Herwig/Pythia	1.0
	Trig. Efficiencies	0.34
	Lepton ID	0.33
	z_0 Efficiency	0.31
Total		36.8

Table 21: Final systematic uncertainties in the calculation of the $W^{\pm}+b\bar{b}$ cross-section.

References

[1] J. Huston, J. Campbell, *Method 2 at NLO*, CDF Note 6849

[2] M.Soderberg, S. Miller, D. Gerdes, *Measurement of* $\frac{W^{\pm}+b\bar{b}}{W^{\pm}+1,2j}$ *in* $W^{\pm}$*+1,2 Jet Events*,CDF Note 7565

[3] M. Soderberg, D. Gerdes, C. Neu, $W^{\pm}+b\bar{b}$ *Acceptance and Pretag Event Selection*,CDF Note 8180

[4] M.L. Mangano, M. Moretti, F. Piccinini, R. Pittau, A. Polosa, *ALPGEN, a generator for hard multiparton processes in hadronic collisions*, JHEP 0307:001,2003,hep-ph/0206293

[5] M. Mangano, M. Moretti, R. Pittau, *Multijet Matrix Elements and Shower Evolution in Hadronic Collisions: $Wb\bar{b}+n$ Jets as a Case Study*, hep-ph/0108069

[6] H. Bachacou, D. Ferretti, J. Nielsen, W. Yao, *Heavy Flavor Contributions to the SECVTX-tagged W+Jets Sample*,CDF Note 7007

[7] S. Budd *et. al*, *Measurement of the t-tbar Production Cross Section in SECVTX-Tagged Lepton+Jets Events*, CDF Note 8037

[8] F. Garberson, S. Grinstein, J. da Costa, C. Hill, A. Holloway, D. Jeans, C. Neu, D. Sherman, *Combination of the SECVTX b-Tagging Scale Factors for Winter 2006 Analyses*, CDF Note 8025

[9] T. Wright, *SecVtx B-Tag Efficiency using Muon Transverse Momentum*, CDF Note 7448